

# INFLUENCE OF PORE SIZE DISTRIBUTION OF ALUMINA BRICK ON COLD CRUSHING STRENGTH BY GREY SYSTEM THEORY

Xueqing Yang <sup>1</sup>, Chengji Deng <sup>1</sup>, Hongxi Zhu <sup>1</sup>, Chao Yu <sup>1</sup>, Jun Ding <sup>1</sup>, Guodong Fan<sup>2</sup>, Guanghui Leng<sup>2</sup>

(1 The State Key Laboratory of Refractories and Metallurgy, Wuhan University of Science and Technology, Wuhan, P.R China)

(2 Henan Dongda High Temperature and Energy Saving Material Co., Ltd, Hebi, P.R. China)

## Abstract

Influence of pore size distribution of alumina brick on its cold crushing strength (CCS) at room temperature was studied by grey system theory. The pore size distribution of specimens was characterized by mercury intrusion porosimetry (MIP), and CCS was tested by universal strength tester. The results show that the pore size distribution of alumina brick was not homogeneous, though the apparent porosity (A.P.) almost no difference. The lesser difference of pore size distribution of specimens contributed immeasurably to dispersion of CCS. The content of pore <15 $\mu$ m had a greater influence on CCS than other pore structure parameters.

## Keywords

- Alumina brick
- Pore size distribution
- Cold crushing strength
- Dispersion.

## INTRODUCTION

Refractory materials are supposed to be resistant to heat and are exposed to different degrees of mechanical stress and strain, corrosion from liquids and gases, and mechanical abrasion at high temperature. They are designed and manufactured so that the properties of the refractories will be appropriate for their applications. Refractories products are highly heterogeneous ceramics, multi-phase, with a coarse skeleton connected by matrix <sup>[1]</sup>.

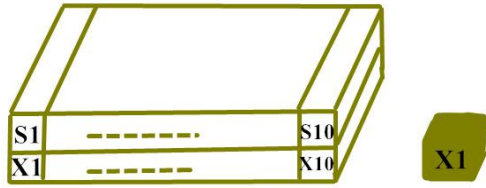
The high-alumina brick is the most widely used and long historically researched refractory products, with high refractoriness, high resistance to acid and alkali slag erosion, high mechanical strength and good cost performance<sup>[2]</sup>. Generally, the brick is constituted by three grades of coarse, medium and fine particles, bound by the pulp waste, used a press (friction press or hydraulic press) one-way compression molding. After sintering in this process, there has a high porosity (about 20%), and the pores distribute unevenly along the direction of the molding pressure.

The strength of a refractory material is an indication of its suitability for use in construction. It is a combined measure for the strength of the grains and also of the bonding system. There is a common fact that CCS of high alumina standard brick in the different parts has large fluctuation. But the existing researches on the mechanical properties of high alumina bricks mainly focus on the phase composition, sintering temperature, grain size, combination ways and et al. of materials <sup>[3-4]</sup>. A small number of researches have been done to investigate the relationship between pore structure and strength of refractories <sup>[5-7]</sup> and few researches have been done about the dispersion of strength in an individual brick.

In the concrete belonged to the silicate system as the refractory material, some researchers have studied the pore structure parameters and strength and durability of the concrete by means of grey relational theory<sup>[8-9]</sup>. In this paper, pore size distributions and complexity of pore morphology had been investigated to find the relationship between pore structure parameters and the dispersion of CCS. The correlation coefficient between the pore structure parameters and the strength was obtained by using the grey theory.

## EXPERIMENTAL PROCEDURE

Specimens in this study were cutted in cube of 25( $\pm$ 2) mm from alumina brick LZ-65, and have been marked as Fig.1. The cold crushing strength (CCS) of specimens had been tested according to GB/T5072-2008. The apparent porosity (A.P.) and bulk density (B.D.) of specimens had been tested according to GB/T2997-2000. The pore size distribution of specimens had been tested by the mercury porosimeter IV9510 according to YB/T118-1997. The chemical and phase compositions were determined by inductively coupled plasma atomic emission spectrometry (ICP-AES). The content of amorphous was obtained by analyzing and calculating of the residue after the HF acid treatment. The cutted specimens were polished to keep the surface smooth to reduce the interference of external factors on test results. Physical properties of specimens had been tested and the results were as follows.



S: A series of specimens at the first layer of alumina brick  
 X: A series of specimens at the second layer of alumina brick  
 Fig.1 Schematic diagram of sample numbers of alumina brick

### EXPERIMENTAL RESULTS AND DISCUSSION

In this experiment brick, the main crystal phases were corundum and mullite. The direct bonding degree of the crystal phases was high, and the network structure was interwoven into a chain. Owing to the strong connection structure and relatively lower content of amorphous, the refractoriness under load was high, creep properties and thermal shock performance were good too. The main chemical and phase compositions of LZ-65 brick were listed in table 1.

Tab. 1 Main chemical and phase compositions of LZ-65 brick

	SiO <sub>2</sub>	Al <sub>2</sub> O <sub>3</sub>	Mullite	Corundum	Cristobalite	Amorphous
Wt./%	12.32	81.8	32	53.5	1.5	13

### PHYSICAL PROPERTIES CHARACTERIZATION

#### (1) Cold crushing strength (CCS)

The histogram of CCS of specimens was shown in Fig. 2. As can be seen from the graph, the average CCS of the 20 specimens was 136.1 MPa. All this 20 strength values are scattered. The CCS of S4 was the minimum deviated from the mean value of 17.0%, S2 was the maximum deviated from the mean value of 27.0%.

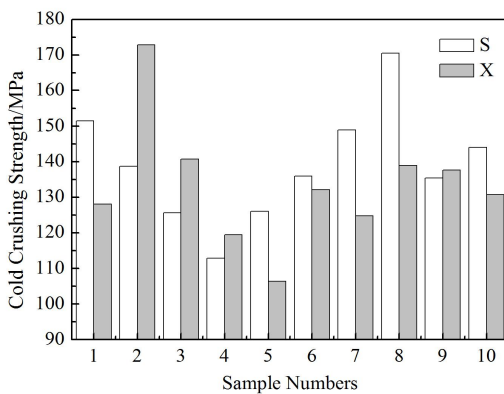


Fig. 2 CCS of all specimens of LZ-65 brick

#### (2) Apparent porosity (A.P.) and bulk density (B.D.)

The porosity in LZ-65 brick was evenly distributed, and the

maximum deviation of 20 specimens was not more than 0.51%. The A.P. and B.D. of the five specimens randomly selected in team X were listed in the table 2. It showed that the average porosity of specimens was 18.85% and the bulk density was 2.868 g.cm<sup>-3</sup>.

Tab. 2 Apparent porosity and bulk density of specimens

Sample number	Apparent porosity /%	Bulk density / (g.cm <sup>-3</sup> )
X2	18.60±0.10	2.872±0.007
X4	18.82±0.11	2.871±0.014
X5	18.91±0.34	2.868±0.014
X7	18.89±0.14	2.862±0.018
X9	18.16±0.42	2.877±0.010
Average	18.85	2.868

### PORE SIZE DISTRIBUTIONS

Fig. 3 was the pore size distributions of 5 specimens, it showed that the first lower peak appears at 3~4μm and the second higher peak appears at 8~12μm. The upper right graph was an enlarged view of the elliptical region, which was the pore size distributions of the specimens at the pore size of 9~14μm. The corresponding peak of X2 is the highest and the peak corresponds to the largest area.

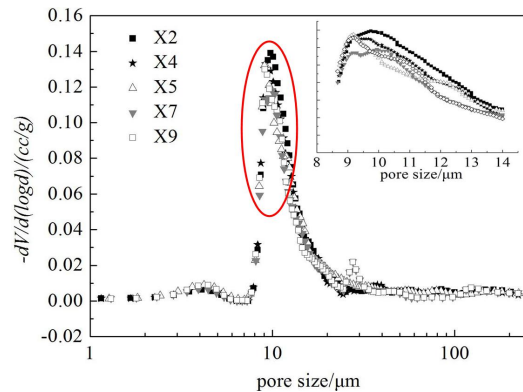


Fig. 3 Pore size distributions of specimens of LZ-65 brick

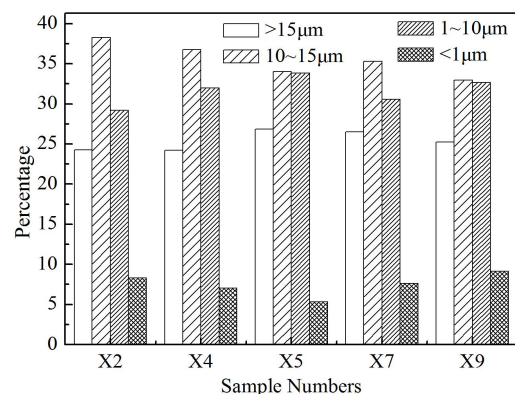


Fig.4 Percentage of four scopes of pore size distributions

Fig. 4 was the histogram of the percentage of four scopes of pore size distributions of the specimens. It showed that the content of pore  $>15\mu\text{m}$  increases slightly from X2 to X9, while the content of pore  $10\sim 15\mu\text{m}$  slightly decreased, the most obvious change was the content of pore  $1\sim 10\mu\text{m}$  increasing first and then had a slight decrease, the content of pore  $<1\mu\text{m}$  decreased first and then increased.

### GREY CORRELATION COEFFICIENT

In order to determine the effect of the pore size distribution parameters on the CCS, the original data of the pore size distribution parameters of the selected specimens were listed in table 3, and the gray correlation coefficient was calculated and analyzed. Detailed calculation method saw the literature<sup>[10]</sup>.

Tab. 3 Pore size distribution parameters and CCS of specimens

Parameters	X2	X4	X5	X7	X9
most probable pore size/ $\mu\text{m}$	9.6	9.4	9.4	10.1	9.0
$>15\mu\text{m}$	24.28	24.20	26.84	26.51	25.26
$10\sim 15\mu\text{m}$	38.25	36.78	34.00	35.29	32.96
$1\sim 10\mu\text{m}$	29.19	31.98	33.85	30.57	32.65
$<1\mu\text{m}$	8.28	7.04	5.31	7.63	9.13
CCS/MPa	172.9	119.5	106.4	124.7	137.7

Table 4 was the gray correlation coefficient of the pore size distribution parameters and CCS. According to the gray correlation coefficient results, in the high alumina brick LZ-65, the content of pore  $<1\mu\text{m}$  made greatest contribution to dispersion of CCS, followed by the content of pore  $10\sim 15\mu\text{m}$ . It can be seen that CCS was more closely related to the content of pore  $<15\mu\text{m}$ .

Tab. 4 Grey relational coefficients between pore size distribution parameters and CCS

Parameters	Correlation coefficient
most probable pore size/ $\mu\text{m}$	0.6047
$>15\mu\text{m}$	0.5558
$15\sim 10\mu\text{m}$	0.6763
$1\sim 10\mu\text{m}$	0.5297
$<1\mu\text{m}$	0.7181

### CONCLUSIONS

When the distribution of porosity in the high alumina brick is uniform, the internal pore size distributions were still quite different, and the macroscopic reaction of CCS was scattered.

Through the gray correlation analysis, it was known that the content of pore  $<15\mu\text{m}$  has a greater influence on CCS. It was helpful to improve the stability of CCS by strictly controlling the content and proportion of pore  $<15\mu\text{m}$  in the preparation process.

### ACKNOWLEDGEMENTS

This work was supported by projects of the National Natural Science Foundation of China (51574187) and International Cooperation Project (2015DFR50800).

### REFERENCES

- [1] Sadik C, Amrani IEE, Albizane A. Recent advances in silica-alumina refractory: A review. *J Asian Ceram Soc.* 2014 Mar 20;2(2): 83-96.
- [2] Auerkari P. Mechanical and physical properties of engineering alumina ceramics. *Sci Sinter.* 2012 Jun;(44): 25-33.
- [3] Zhang X, Yang D. Evaluation on compressive strength and workability of green high-performance concrete by grey relational grade. *Appl Mech Mater.* 2013 Oct 15;(438-439): 166-169.
- [4] Wang J. Effect of microstructure on performance of refractories. *Chin Ceram Soc.* 2002 Jan 28;(6):3-7.
- [5] Sun L, Bao Y. Fracture Behavior and strength evaluation of engineering ceramics. *Adv Ceram.* 1999 Nov 15;(4): 17-21.
- [6] Zhu B, Wei G, Li X, Song Y. Preparation and properties of corundum based microporous refractory. *J Chin Ceram Soc.* 2013 Feb 28;41(3): 422-426.
- [7] Zhu B, Fang B, Li X, Yu D, Jiang X. Influence of pore structure parameters on properties of refractory castables. *Refract.* 2010 Feb 15;44(1): 63-66.
- [8] Al-Amoudi O, Al-Kutti W, Ahmad S, Maslehuddin M. Correlation between compressive strength and certain durability indices of plain and blended cement concretes. *Cem Concr Compos.* 2009 May 21;31(9): 672-676.
- [9] Su X, Sun H. The evaluation to influence factors of concrete durability based on grey correlation degree method. *Adv Mater Res.* 2014 Jul 16;(989-994): 2688-2692.
- [10] Song Y, Deng C, Zhu H, Ding J, Zhang X, Yuan W. Correlation between porosity characteristics and cold crushing strength of forsterite porous materials based on grey system theory. *J Chin Ceram Soc.* 2016 Jun 15;44(6): 896-900.